



DEPENDENCE OF OPTICAL PROPERTIES ON STRUCTURAL PARAMETERS OF MULTIPLE QUANTUM WELL EMBEDDED IN ACTIVE REGION OF VCSEL

Krishanu Nandy¹, Suhrid Biswas¹, Rahul Bhattacharyya¹, Arpan Deyasi²

¹U.G student, Dept. of Electronics & Communication Engineering,
RCC Institute of Information Technology, Kolkata-700015

²Assistant Professor, Dept. of Electronics & Communication Engineering,
RCC Institute of Information Technology, Kolkata-700015

Received 12-04-2013, online 23-04-2013

ABSTRACT

Reflection coefficient and full-width-half-maximum (FWHM) of a vertical cavity surface emitting laser are numerically computed by independently varying the well and barrier dimensions and material composition of the barrier layer of the multiple quantum well embedded in the active region of the device. Reflection coefficient is calculated as a function of operating wavelength considering 1550 nm as central value for optical communication using propagation matrix method. Refractive indices of the MQW materials are considered as function of bandgap, operating wavelength and material composition following Adachi's model. The notable feature arises from the analysis is that suitable tuning of structural parameters can make it a bandpass or bandreject filter, which can be quantitatively computed from magnitude of FWHM. A nanometer bandwidth speaks for bandpass filter, whereas picometer range tells for its band-reject characteristics. No. of layers in the MQW also controls the filter characteristics. Simulated results can be utilised to design VCSEL as optical transmitter in desired spectrum.

Keywords: Bragg Reflection, Reflectivity, Multiple Quantum Well, Band-reject Filter, Full-Width-Half-Maximum.

I. INTRODUCTION

Vertical cavity laser has the potential advantage compared with the other quantum well lasers that it possesses surface emitting characteristics, and therefore, can be well suited for spectroscopy, storage and medical applications. It has the potential advantage of narrow beam divergence when efficiently coupled with optical fiber, single mode operation due to very short effective cavity length, low power consumption and low cost manufacturability. Its working is based on the quarter-wave Distributed Bragg Reflector

principle which can effectively be utilized in lightwave communications [1-2]. Usually multilayer semiconductor heterostructures are used to consider the effect of light absorption on optical properties of Bragg reflectors [3]. Recently, researchers [4] proposed that devices with nitride based materials are promising optical emitters in UV range, which is required for high-speed optical communication [5-7] and higher information capacity [8-11] with low-loss and low-dispersion fiber transmission window from 1470 nm to 1610 nm [12-13]. In a VCSEL, electromagnetic wave resonates between mirrors

on the top and bottom surfaces so that the photons pass through only a very short length of active medium for stimulating emission process. Hence reflection coefficient and full-width-half-maximum become the two critically important optical parameters for its design at 1550 nm wavelength. Structural parameters of the multiple quantum well in active region have a crucial say in this regard.

Iga [14] first proposed the idea of VCSEL, which was successfully demonstrated [15] for CW-wave room temperature operation. Due to its higher efficiency [16] and ultralow threshold current [17-18], it is used in CWDM optical-network applications. Hence efficient optimization is required for design of VCSEL with high performance [19]. Hence, by suitably choosing the refractive indices of the constituting layers along with dimension of MQW structure placed inside active region, required filter characteristics can be obtained when calculated at the desired frequency region. Bandwidth of the filter can be quantitatively measured by computing FWHM, which speaks about pass-band/reject-band filter.

In this paper, reflectivity of 11-layer VCSEL structure is calculated by varying the dimension of the barrier and well thicknesses of the multiple quantum well structure, and also by varying the material composition of the barrier layer. Corresponding FWHM is calculated and plotted to estimate the bandwidth variation. Number of layers inside the MQW is also varied to get the change in FWHM. GaN/Al_xGa_{1-x}N

material composition is considered for simulation purpose. Simulation results will help the engineers to design efficient VCSEL for required communication applications.

II. MATHEMATICAL MODELING:

We consider the simplest three layers having refractive indices as shown in Fig 1:



Fig 1: Three-layer interface with refractive indices n_1, n_2, n_1

We consider wavevectors k_0, k_1, k_2 defined as in terms of wavelength, and assume normal incidence of light on the structure. For wave at media interface having propagation constant k_1 and k_2 respectively, satisfaction of boundary conditions give the following equation-

$$A_1 \exp(-ik_1 z) + A_2 \exp(ik_1 z) = B_1 \exp(-ik_2 z) + B_2 \exp(ik_2 z) \quad (1)$$

If we consider the simplest three layers having refractive indices as shown in Fig 1, then interface matrices can be computed as follows:

$$[D0] * [\text{input from air}] = [D1] * [\text{output to } n1],$$

$$[D1] * [\text{input from } n1] = [D2] * [\text{output to } n2]$$

The interface matrices, which is a function of the propagation vector, can in general be represented as-

$$D_i = \begin{bmatrix} 1 & 1 \\ k_i & -k_i \end{bmatrix} \quad (2)$$

where

$$k_i = \frac{2\pi}{\lambda} n_i \quad (3)$$

n_i is the refractive index of the i^{th} layer. Considering propagation of electromagnetic wave from left to right, propagation matrices P_1, P_2, P_3 in general can be written as

$$P_i = \begin{bmatrix} \exp(-jk_i d_i) & 0 \\ 0 & \exp(jk_i d_i) \end{bmatrix}. \quad (4)$$

Gain can be calculated as-

$$G_i = (D_i P_i (D_i)^{-1}) (D_{i+1} P_{i+1} (D_{i+1})^{-1}) \quad (5)$$

where G_1 gives the gain for lower mirror, and G_2 gives it for upper mirror. Wave propagation through the lower and upper layers for N no. of wells is given by

$$L = (D_0^{-1})(G_1^N)(D_1) \quad (6.1)$$

$$U = (D_1^{-1})(G_2^N)(D_0). \quad (6.2)$$

Total propagation is given by

$$T = L * P_3 * U. \quad (7)$$

Reflected electromagnetic field (r) is obtained by dividing the $T(2,1)$ by $T(1,1)$. Total reflection intensity is given by

$$R = r.r^* . \quad (8)$$

FWHM can be calculated from the knowledge of R . It can be accurately predicted when there exists one peak in the range. For that purpose, maximum of R is first obtained, and set the convergence condition such that

$$R < (\max(R))/2 \quad (9)$$

For calculation of refractive index of all nitrides material, we consider the working formula

proposed by Adachi and later simplified by several researchers [20-21] is given below:

$$n(E) = \sqrt{A \left(\frac{\hbar\omega}{E_g}\right)^{-2} \left\{ \begin{array}{l} 2 - \sqrt{1 + \left(\frac{\hbar\omega}{E_g}\right)} \\ - \sqrt{1 - \left(\frac{\hbar\omega}{E_g}\right)} \end{array} \right\} + B} \quad (10)$$

where E_g is the bandgap energy of the material, ω is the frequency of the laser emission and A and B are the fitting parameters. For simulation purpose, we have considered GaN/Al_xGa_{1-x}N composition.

III. RESULTS AND DISCUSSION:

Using the equations derived earlier, reflection coefficient of a VCSEL is calculated considering the 11-layer MQW structure embedded inside the active region of the cavity. Operating wavelength is taken as 1.55 μm , and reflectivity of the structure is plotted and shown in Fig 2. In Fig 2a, it may be seen that the device acts as a bandpass filter for Al_{0.4}Ga_{0.6}N/GaN composition, as its reflectivity is very low in the desired operating region. But if the Al concentration is slightly increased, then at a critical value of x , the filter becomes a band-reject one. This is due to the fact that by increasing the Al content in barrier region, bandgap of the material increases, which decreases the refractive index of that layer; and thus the difference of refractive index between the well and barrier regions increases. When this difference exceeds a critical value, the

reflectivity starts to change in reverse direction, i.e., the decreasing trend is now becomes a rise in magnitude. This ensures the fact that a proper choice of material composition of the MQW structure is very important in designing VCSEL keeping the layer widths and no. of layers constant.

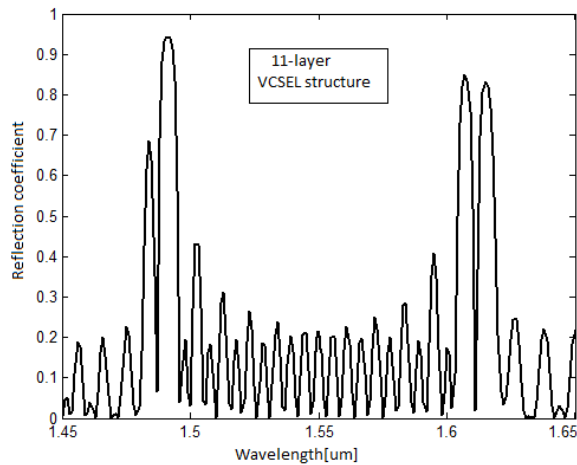


Fig 2(a): Reflection coefficient with wavelength for 11-layer VCSEL with $Al_{0.4}Ga_{0.6}N/GaN$ composition

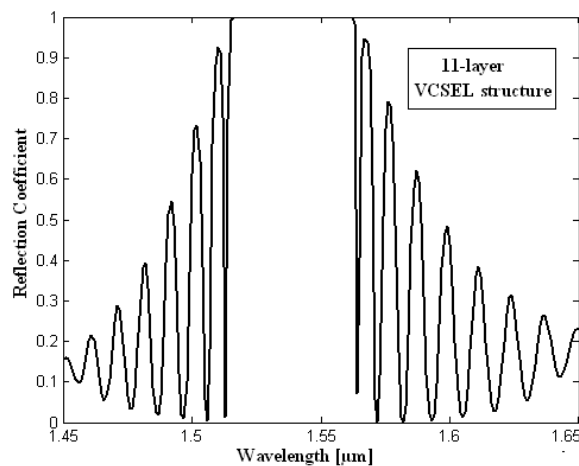


Fig 2(b): Reflection coefficient with wavelength for 11-layer VCSEL with $Al_{0.6}Ga_{0.4}N/GaN$ composition

Filter characteristics can also be tuned by varying the well or barrier layer thicknesses, shown in Fig 3. In Fig 3a, it is observed that the device will behave as band-reject filter for 3.5

μm barrier thickness, but slight tuning of the dimension in either direction changes its profile so that it becomes a bandpass one. This bandwidth can be altered by varying well width also keeping barrier width constant, plotted in Fig 3b. From the Fig, it is found out that for 2.7 μm well width; the filter exhibits band-reject property, whereas it tends to show the bandpass property when well dimension slightly deviates from the critical value.

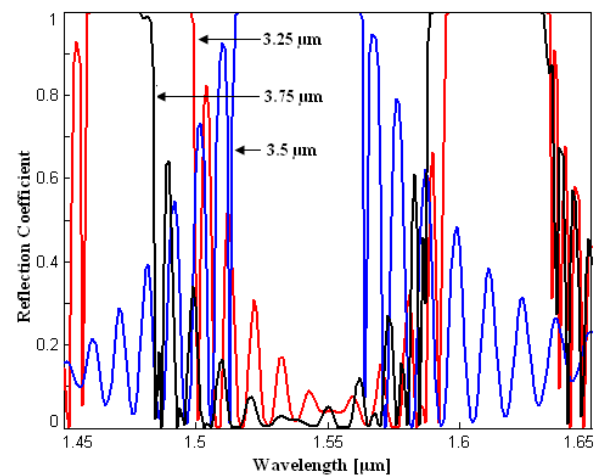


Fig 3(a): Reflection coefficient with wavelength for different barrier thickness of MQW structure

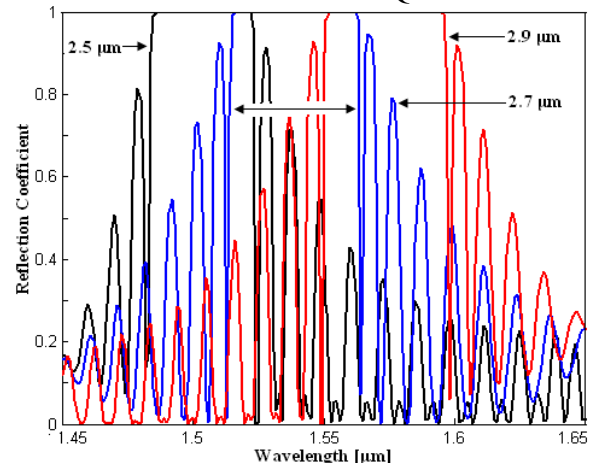


Fig 3(b): Reflection coefficient with wavelength for different well thickness of MQW structure

Fig 4 shows the variation of full-width at half-maximum profiles against the variation

of different structural parameters of the MQW embedded in the active region of the device. Fig. 4a gives the variation with material composition of the barrier layer. From the plot, it can be seen that for a range of Al composition (x), FWHM is high (~ 2 nm); whereas it decreases and almost attains zero ($< \text{pm}$) for some particular value of x . The reason behind the oscillatory nature is that when the structure behaves as a bandpass filter, its FWHM becomes high. But when it is tuned band-reject one, FWHM reduces with a very high rate, and almost attains minimum value. This also validates the earlier obtained result. For $\text{Al}_{0.4}\text{Ga}_{0.6}\text{N}/\text{GaN}$ composition, the structure exhibits bandpass characteristics, whereas for $\text{Al}_{0.6}\text{Ga}_{0.4}\text{N}/\text{GaN}$ composition, it shows band-reject behavior. This is verified in Fig 4a. Variation of FWHM is plotted with barrier thickness in Fig. 4b. From the plot, it is observed that for some particular range of barrier thickness, it behaves as bandpass one, whereas for other values, it turns to the band-reject filter. Data obtained from the plot supports the result obtained and graphically represented in Fig .3a. The same property holds when well thickness is varied and corresponding FWHM is plotted, as displayed in Fig. 4c. Henceforth, one can quantitatively understand the nature of filter from FWHM profile, which depends on structural parameters of multiple quantum well.

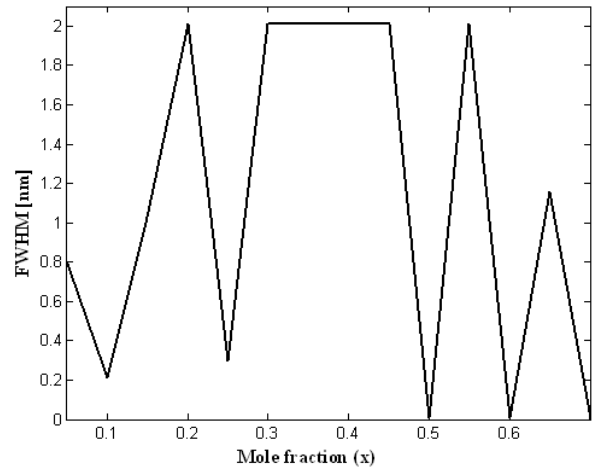


Fig 4a: FWHM with Al mole fraction (x) for 11-layer structure

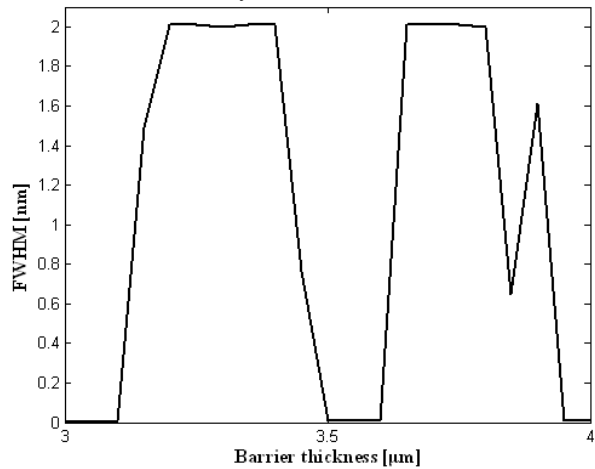


Fig 4b: FWHM with barrier layer width of MQW structure for 11-layer structure

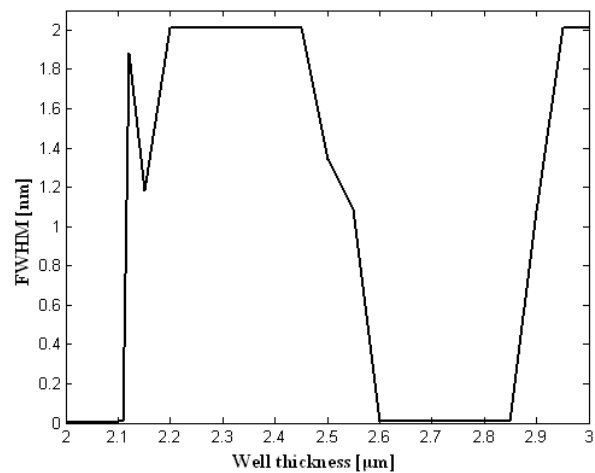


Fig 4c: FWHM with well thickness of MQW structure for 11-layer structure

By increasing number of layers, it is seen that FWHM becomes almost constant upto a critical value ($N=24$), and then it suddenly increases, and then decreases to almost zero. This is plotted in Fig 5. This is due to the fact that for a specified wavelength range with a given structural set of parameters, the filter behaves as bandpass filter, and then passband width increases for a particular value of layer number. Further increase of N makes the device as band-reject filter, for which FWHM drastically decreases.

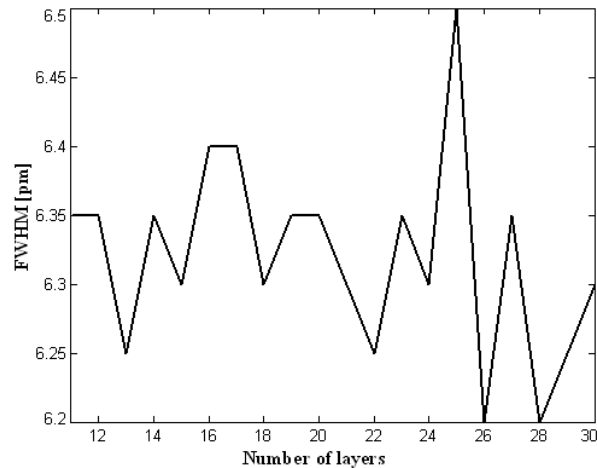


Fig 5: FWHM with no. of layers of MQW structure

IV. CONCLUSION

Reflection coefficient of a VCSEL is numerically calculated and plotted with different structural parameters of the multiple quantum well placed in the active region (in between two mirrors) of the laser and corresponding FWHM is estimated. For certain set of physical parameters of the MQW, the device behaves as bandpass filter, whereas it can be tuned into band-reject one by changing the dimensions or material composition of well and barrier layers.

FWHM of the device becomes of the order of nm, when it acts as a passband filter, whereas for rejection bandwidth, it becomes less than pm length. For all the calculations, 1550 nm is considered as central wavelength of operation for the sloe purpose of using the device in optical communication. Optimized results are very helpful from design engineer's perspective of making vertical cavity surface emitting laser for specific requirement.

References

1. M. Linnik and A. Christou, "Effects of Bragg Mirror Interface Grading and Layer thickness Variations on VCSEL Performance at 1.55 μm ", Proceedings of SPIE, 4286, 162 (2001).
2. T. Saka, M. Hirotsu, T. Kato and H. Susava, "Bragg Reflector of GaAlAs/AlAs Layers with Wide Bandwidth Applicable to Light Emitting Diodes", Journal of Applied Physics, **73**, 380 (1993).
3. A. V. Kavokin and M. A. Kaliteevski, "Light Absorption Effect on Bragg Interference in Multilayer Semiconductor Heterostructures", Journal of Applied Physics, **79**, 595 (1996).
4. C. Alhenc-Gelas, P. Heroin, M. Abid, J. Jacquet, S. Gautier and A. Ougazzaden, "Design Rules of high reflectivity Bragg GaAlN Mirrors for 300 nm VCSEL's", Proc of SPIE, 7229, 72290N (2009).
5. E.B. Grann, K. Herry, B.C. Peters, and B. Wiedemann, "Datacom Applications for New VCSEL Technologies", in Vertical-Cavity

Surface-Emitting Lasers-IV, Proceedings of SPIE 3946, 165 (2000).

6. I.H. White, M. Webster, and R.V. Penty, "High Bandwidth Optical Links over Multimode fibre", in Proceedings of IEEE Lasers and Electro-Optic Society Annual Meetings, LEOS, 2, 695, San Francisco, CA, USA, Nov. 1999.

7. R. Michalzik, P. Schnitzer, U. Fiedler, D. Wiedenmann, and K.J. Ebeling, "High-bit-rate Data Transmission with Short-Wavelength Oxidized VCSEL's: Toward Bias-free Operation", IEEE Journal of Selected Topics on Quantum Electronics, **3**, 396 (1997).

8. L.B. Aronson, B.E. Lemo, L.A. Buckman, and D.W. Dol, "Low-cost Multimode WDM for Local Area Networks up to 10 Gb/s", IEEE Photonics Technology Letters, **10**, 1489 (1998).

9. X. Zhao and F.-S. Choa, "10 Gb/s Multimode Fiber Transmissions over any (loss-limited) Distances Using Adaptive Equalization Techniques", Proceedings of 26th European Conference on Optical Communication, ECOC, 3, 57, Munich, Germany, Sept. 2000.

10. R. Michalzik, G. Giaretta, A.J. Ritger, and Q.L. Williams, "10 Gb/s VCSEL-based Data Transmission over 1.6km of New Generation 850nm Multimode fiber", IEEE Lasers and Electro-Optic Society Annual Meetings, LEOS, PD1.6. San Francisco, CA, USA, Nov. 1999.

11. U. Fiedler, G. Reiner, P. Schnitzer, and K.J. Ebeling, "Top-Surface Emitting Vertical-Cavity Laser Diodes for 10 Gbit/s Data Transmission", IEEE Photonics Technology Letters, **8**, 746 (1996).

12. T. Marozsák and E. Udvary, "Vertical Cavity Surface Emitting Lasers in Radio over Fiber Applications", J. of Telecommunications and Information Technology, **1**, 36 (2003).

13. D. Wiedenmann, R. King, C. Jung, R. Jager, R. Michalzik, P. Schnitzer, M. Kicherer and K. Ebeling, "Design and Analysis of Single-Mode Oxidized VCSEL's for High-Speed Optical Interconnects", IEEE Journal of Selected Topics in Quantum Electronics, **5**, 503 (1999).

14. H. Soda, K. Iga, C. Kitahara, and Y. Suematsu, "GaInAsP/InP Surface Emitting Injection Lasers", Japanese Journal of Applied Physics, **18**, 2329 (1979).

15. K. Iga, S. Ishikawa, S. Ohkouchi, and T. Nishimura, "Room-Temperature Pulsed Oscillation of GaAlAs/GaAs Surface-Emitting Injection Laser", Applied Physics Letters, **45**, 348 (1984).

16. B. Weigl, M. Grabherr, G. Reiner, and K. J. Ebeling, "High Efficiency Selectively Oxidized MBE Grown Vertical-Cavity Surface-Emitting Lasers", Electronics Letters, **32**, 557 (1996).

17. M. H. MacDougal, P. D. Dapkus, V. Pudikov, H. Zhao, and G. M. Yang, "Ultralow Threshold Current Vertical-Cavity Surface Emitting Lasers with AlAs-Oxide-GaAs Distributed Bragg Reflectors", IEEE Photonics Technology Letters, **7**, 229 (1995).

18. Y. Hayashi, T. Mukaiharu, N. Hatori, N. Ohnoki, A. Matsutani, F. Koyama, and K. Iga, "Record Low-Threshold Index-Guided InGaAs/GaAlAs Vertical-Cavity Surface-Emitting Laser with a Native Oxide

Confinement Structure,” *Electronics Letters*, **31**, 560 (1995).

19. J. C. Cartledge and R. C. Srinivasan, “Extraction of DFB Laser Rate Equation Parameters for System Simulation Purposes”, *Journal of Lightwave Technology*, **15**, 852 (1997).

20. M. Gudan, J. Piprek, “Material Parameters of Quaternary III-V Semiconductors for Multilayer Mirrors at 1.55 micron wavelength”, *Modeling and Simulation of Material Science Engineering*, **4**, 349 (1996).

21. G. M. Laws, E. C. Larkins, I. Harrison, C. Molloy, D. Somerford, “Improved Refractive Index Formulas for the AlGaN and InGaN Alloys”, *Journal of Applied Physics*, **89**, 1108 (2001).